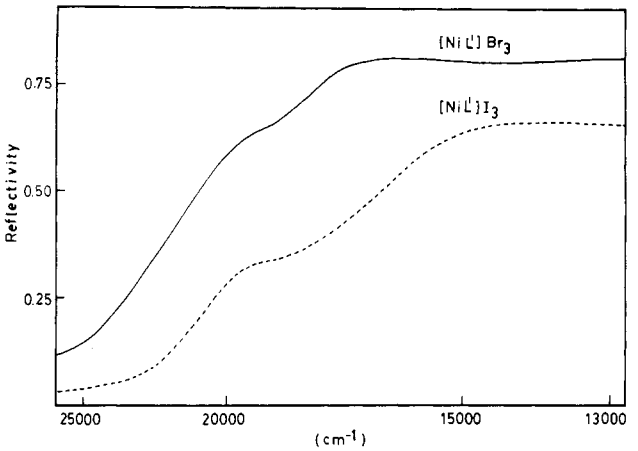


**Figure 9.** Reflectance spectra of $[NiL^1]X_3$ (X = Br, I).

trihalide ions, which appear as the counteranions of the complex ion $[NiL^1]^+$.

Both $[NiL^1]Br_3$ and $[NiL^1]I_3$ are diamagnetic substances; they are also EPR-silent, and therefore they are neither Ni(III) species nor octahedral Ni(II) complexes.

The reflectance spectra of $[NiL^1]X_3$ contain intense bands of counteranions throughout the blue end of the visible region and a shoulder for $[NiL^1]^+$ ion at ca. 18 800 $cm^{-1}$ (Figure 9). The absorption at 18 800 $cm^{-1}$ is considerably lower in energy than those observed for a large number of the planar diamagnetic tetraamine complexes whose band maxima usually fall in the range 25 000–20 500 $cm^{-1}$. From this and the presence of a coordinated carboxylate group in $[NiL^1]X_3$, it is evident that the geometry of $[NiL^1]X_3$ about the metal ions is nonplanar. Low-spin five-coordinate nickel(II) complexes usually have only one absorption spectrum in the visible region, generally in the range 20 000–16 660 $cm^{-1}$.[20] The reflectance spectra for the complexes $[NiL^1]X_3$ indicate that they might have a low-spin five-coordinate structure. This is a rare case for such complexes that contain a pendent tetraazamacrocyclic ligand and a trihalide counteranion. More efforts will be yet required to elucidate this phenomenon.

**Acknowledgment.** This research was supported by a grant from the Science Foundation of Academia Sinica. We are indebted to Professor Thomas A. Kaden for a helpful discussion.

**Supplementary Material Available:** Listings of anisotropic thermal parameters, the derived hydrogen positions, all nonessential bond lengths and angles, and least-squares planes and deviations therefrom for compounds **1**, **3**, and **6** (11 pages); tables of calculated and observed structure factors for the three compounds (80 pages). Ordering information is given on any current masthead page.

(20) Furlani, C. *Coord. Chem. Rev.* **1968**, *3*, 141.

Contribution from the Department of Chemistry, University of Michigan, Ann Arbor, Michigan 48109-1055

# Vanadium Complexes of the Tridentate Schiff Base Ligand *N*-Salicylidene-*N'*-(2-hydroxyethyl)ethylenediamine: Acid–Base and Redox Conversion between Vanadium(IV) and Vanadium(V) Imino Phenolates

Xinhua Li, Myoung Soo Lah, and Vincent L. Pecoraro*

*Received May 5, 1988*

The reaction of vanadyl sulfate or vanadyl acetonylacetate ($VO(ACAC)_2$) with *N*-salicylidene-*N'*-(2-hydroxyethyl)ethylenediamine ($H_2SHED$) affords a wide range of vanadium(IV) and vanadium(V) complexes. The structure of $V^{IV}O(HSHED)(ACAC)$ was determined by an X-ray analysis of red crystals having the following crystallographic parameters: space group *Pbca* (orthorhombic); $a$ = 11.607 (5), $b$ = 25.960 (2), $c$ = 11.701 (5) Å; $V$ = 3526 (2) Å$^3$; $Z$ = 8. The final $R$ indices were $R$ = 0.051 and $R_w$ = 0.040 for 1485 observed data. The vanadium is six-coordinate with the phenolate, imine, and amine donors of $HSHED^-$ oriented in a meridional geometry. The hydroxyl oxygen remains unbound. The ACAC moiety is a bidentate chelate with one oxygen atom (V1–O5, 2.194 (5) Å) trans to the short V=O bond (V1–O1, 1.596 (4) Å). When the complex is dissolved in methanol, ACAC dissociates from a small fraction of $V^{IV}O(HSHED)(ACAC)$, yielding air-sensitive $V^{IV}O(SHED)$ in which an alkoxide oxygen atom of the ligand has been inserted in the coordination sphere. If this green material is left in air for several days, orange blocks and yellow plates are deposited. X-ray analysis of both crystal types reveals that the two materials are weakly associated solid-state dimers of the pervanadyl–$HSHED^-$ complex $VO_2(HSHED)$, which result from different hydrogen bonding in the crystals. Once again, $HSHED^-$ is a meridional, tridentate chelate with amine, imine, and phenolate ligation. The orange material shows a vanadium–vanadium separation of 3.103 (1) Å and a long V1–O1′ distance of 2.298 (2) Å. In contrast, the yellow crystals reveal a more weakly associated structure with V1–V1′ of 3.251 (1) Å and V1–O1′ equal to 2.455 (2) Å. Acidification of an acetonitrile solution of either the yellow or orange compounds results in the formation of a stable oxo–hydroxo–$V^V$HSHED complex, which is red. Further addition of acid generates the deep blue, highly unstable monoxo–$V^V$HSHED complex. A comparison to related V(IV) and V(V) complexes and the potential biological relevance are discussed. Crystallographic parameters for $[VO_2(HSHED)]_2$ (yellow, **1**): space group $P2_1/c$ (monoclinic); $a$ = 11.246 (3), $b$ = 6.842 (2), $c$ = 17.022 (5) Å; $\beta$ = 114.38 (6)°; $V$ = 1193.0 (6) Å$^3$; $Z$ = 4. The final $R$ indices were $R$ = 0.027 and $R_w$ = 0.027 for 1729 observed data. Crystallographic parameters for $[VO_2(HSHED)]_2$ (orange, **2**): space group $P2_1/c$ (monoclinic); $a$ = 10.249 (2), $b$ = 10.999 (2), $c$ = 10.578 (2) Å; $\beta$ = 119.16 (4)°; $V$ = 1191.6 (4) Å$^3$; $Z$ = 4. The final $R$ indices were $R$ = 0.029 and $R_w$ = 0.029 for 1265 observed data.

## Introduction

Until very recently, the biological chemistry of vanadium had only been established for a novel natural product (amavadin)[1] in the mushroom *A. muscaria*, in the blood of sessile marine organisms known as tunicates,[2] and as a potent inhibitor of phosphoryl transfer enzymes.[3] The latter activity results from the formation of a stable pentacoordinate V(V) species generated as an analogue of the phosphorus transition state.[4,5] Although the chemical structure of amavadin has been elucidated,[6] its function

(1) Bayer, E.; Kneifel, H. *Z. Naturforsch., B: Anorg. Chem., Org. Chem., Biochem., Biophys., Biol.* **1972**, *27B*, 207.
(2) Kustin, K.; McLeod, G. C.; Gilbert, T. R.; Briggs, L.R. *Struct. Bonding (Berlin)* **1983**, *53*, 139.
(3) Cantley, L. C., Jr.; Cantley, L. G.; Josephson, L. *J. Biol. Chem.* **1978**, *253*, 7361.
(4) Alber, T.; Gilbert, W. A.; Ponzi, D. R.; Petsko, G. A. *Ciba Found. Symp.* **1983**, *93*, 4.
(5) Wlodawer, A.; Miller, M.; Sjolin *Proc. Natl. Acad. Sci. U.S.A.* **1983**, *80*, 3628.

0020-1669/88/1327-4657$01.50/0 

is still unknown. In contrast, the composition and solution environment of hemovanadin, which was once thought to act as an oxygen carrier in tunicates, has been the subject of considerable controversy.[7,8] In none of these cases, however, was vanadium an essential component associated with direct enzymatic activity.

It is easy to understand, therefore, the heightened interest in the biological chemistry of vanadium due to the recent discovery of two types of vanadium-dependent enzymes with nitrogenase[9] and bromoperoxidase[10,11] activity. The vanadium nitrogenase may contain a vanadium–iron–sulfur cluster that is a structural analogue of the well-known molybdenum enzyme.[12,13] The bromoperoxidases, which catalyze the reaction shown in eq 1, are thought

$$AH + Br^- + H_2O_2 + H^+ \rightarrow ABr + 2H_2O \qquad (1)$$

to contain a mononuclear vanadium(V) active site.[14] Both mechanistic and biophysical studies are aimed at elucidating the mechanism of bromination of organic substrates by these haloperoxidases.[14,15]

In this contribution we report the structures and physical properties of a full series of vanadium complexes which may provide further insight into the biological chemistry of this element. Vanadium complexes of the ligand *N*-(salicylidene)-*N'*-(2-hydroxyethyl)ethylenediamine, $H_2SHED$, were isolated and characterized by using X-ray crystallography as a *cis*-dioxovanadium(V) dimer, $[VO_2(HSHED)]_2$, and a mononuclear $VO^{2+}$ complex containing acetonylacetonate, [VO(HSHED)(ACAC)]. In addition, mononuclear V(IV) and V(V) complexes, generated by the addition of base or acid, were investigated. Taken together, these materials provide a set of potentially biologically relevant compounds interrelated by acid–base and redox equilibria.

## Materials and Methods

The following abbreviations are used throughout the text: ACAC = 2,4-pentanedionate; $H_2SHED$ = *N*-salicylidene-*N'*-(2-hydroxyethyl)-ethylenediamine; $(TBA)PF_6$ = tetra-*n*-butylammonium hexafluorophosphate; EHPG = ethylenebis[(*o*-hydroxyphenyl)glycinate]; EHGS = ethylene-*N*-[2-(*o*-salicylidineamino)ethyl]-*N'*-(*o*-hydroxyphenyl)-glycinate; SALEN = *N,N'*-disalicylideneethylenediaminate; [9]aneN$_3$ = 1,4,7-triazacyclononane; 8-Q = 8-quinolate.

**Materials.** Salicylaldehyde, *N*-(2-hydroxyethyl)ethylenediamine, $VO(SO_4)_2 \cdot H_2O$, and $VO(ACAC)_2$ were purchased from Aldrich Chemical Co. $(TBA)PF_6$ was made by a metathesis reaction of (TBA)Br and $NH_4PF_6$ and recrystallized from hot ethanol prior to electrochemical studies. Anhydrous HCl in acetonitrile was obtained by bubbling HCl (Matheson Gas) into a vessel containing dried and distilled acetonitrile. High-purity solvents for electrochemical studies were purchased from American Burdick and Jackson Co. and used as received for electrochemical studies. These solvents were stored under argon, which was also used to deaerate solutions. All other chemicals and solvents were reagent grade. Elemental analyses were performed by Galbraith Laboratories, Knoxville, TN.

**Preparation of Compounds.** Unless otherwise indicated all reactions and manipulations were performed under nitrogen atmosphere by using standard Schlenk-line techniques.

**$[VO_2(HSHED)]_2$ (1 and 2).** Salicylaldehyde (2 mL, 18.8 mmol) and *N*-(2-hydroxyethyl)ethylenediamine (1.9 mL, 18.8 mmol) were added to 75 mL of degassed methanol and allowed to react for 1 h. Vanadyl sulfate hydrate (3.74 g, 18.8 mmol), dissolved in 50 mL of degassed water, was added to this solution, and after 3 h, the solution turned blue with a small amount of blue solid precipitating. At this point, NaOH (1.5 g, 37.6 mmol) was added to the mixture, the solution openned to the air, and the reaction stirred overnight. First, a yellow solid precipitated. Both orange blocks of **1** and yellow rectangular crystals of **2** could be recovered upon standing and were separated manually. X-ray structure determination (vide infra) demonstrated that the orange blocks are the dimer **1** while a more weakly associated material is obtained as **2**. The IR spectrum of the orange blocks was similar to but not identical with that of the yellow solid; however, the IR spectra of the yellow rectangles and yellow powder were identical. When the compounds were dissolved in DMSO, the cyclic voltammograms obtained for **1** and **2** and the $^{51}V$ NMR resonances (−529 ppm vs $VOCl_3$) were identical. Similarly, DMF solutions of **1** and **2** showed identical $^1H$ NMR spectra (8.97 ppm (singlet) 1 H, imine; 6.8–7.6 ppm (multiplet) 4 H, phenyl; 5.46 ppm (broad singlet) 1 H, hydroxyl; 4.94 ppm (triplet) 1 H, 4.17 ppm (multiplet) 1 H, 3.97 ppm (multiplet) 1 H; 3.55 ppm (multiplet) 1 H, 3.05 ppm (multiplet) 1 H, 2.94 ppm (singlet) 1 H, and 2.78 ppm (singlet) 1 H, methylene and amine protons). Elemental analyses for both materials are consistent with a formulation $VO_2(HSHED)$. The overall yield of **1** is 35%, and the yield of **2** is 45%. Anal. Calcd for **1** ($C_{22}H_{30}N_4O_8V_2$): C, 45.52; H, 5.17; N, 9.66; V, 17.59. Found: C, 45.60; H, 5.62; N, 9.52; V, 17.52. Anal. Calcd for **2** ($C_{11}H_{15}N_2O_4V$): idetical with that for **1**. Found: C, 45.32; H, 5.35: N, 9.57; V, 17.56.

**[VO(OH)HSHED]Cl (3) and $[VO(HSHED)]Cl_2$ (4).** These complexes can be synthesized in situ but can not be isolated as solids. When 1 equiv of HCl dissolved in anhydrous acetonitrile is added to **2** dissolved in dry acetonitrile, a red solution is generated. A rust-pink solution is generated when acidification is carried out in DMSO. These solutions, which contain **3**, are stable for hours at room temperature open to the air or under inert atmosphere. Addition of an excess of HCl in acetonitrile causes a change from red to deep blue, indicating the formation of the $VO(HSHED)^{2+}$ cation. This material is very unstable, decomposing in a matter of minutes.

**[VO(HSHED)(ACAC)] (5).** Salicylaldehyde (2 mL, 18.8 mmol) and *N*-(2-hydroxyethyl)ethylenediamine (1.9 mL, 18.8 mmol) were added to a 250-mL flask containing 150 mL of degassed methanol. After this mixture was heated at reflux for 1 h and cooled to room temperature, vanadyl acetonylacetonate (2.49 g, 9.4 mmole) was added. The clear red solution that was generated was refluxed overnight under nitrogen. The volume was reduced to half by using a Schlenk line. When the solution was allowed to stand, X-ray quality square red prisms were collected. Quantitative production of **1** can be accomplished if the red solution is allowed to stand in air for several days. Yield: 80%. Anal. Calcd for $C_{16}H_{22}N_2O_5V$: C, 51.48; H, 5.90; N, 7.51; V, 13.67. Found: C, 51.37; H, 5.97; N, 7.48; V, 13.62.

**[VO(SHED)] (6).** This material may be generated in two ways. (A) **5** (1.43 g, 0.38 mmol) was added to 100 mL of degassed methanol, and then sodium methoxide ((0.21 g, 0.38 mmol) was added. The red solution was refluxed under nitrogen for 4 h and then sealed for several days. A microcrystalline, air-sensitive green solid (**6**) was recovered. (B) Salicylaldehyde (2 mL, 18.8 mmol) and *N*-(2-hydroxyethyl)ethylenediamine (1.9 mL, 18.8 mmol) were added to a 250-mL flask containing 150 mL of degassed methanol. After the mixture was heated at reflux for 1 h under nitrogen, vanadyl acetonylacetonate (4.99 g, 18.8 mmol) followed by sodium methoxide (1.02 g, 18.8 mmole) was added and the solution refluxed overnight. The solution was allowed to stand, giving a microcrystalline green powder. Yield: method A, 60%; method B, 70%. Anal. Calcd for $C_{12}H_{18}N_2O_4V$: C, 47.21; H, 5.90; N, 9.18; V, 16.72. Found: C, 47.06; H, 5.55; N, 9.17; V, 16.60.

**Collection and Reduction of X-ray Data.** Suitable crystals of $VO_2$-(HSHED), $[VO_2(HSHED)]_2$, and [VO(HSHED)(ACAC)] were obtained as described above. These crystals were mounted in glass capillaries. Intensity data were obtained at room temperature on a Syntex $P2_1$ diffractometer using Mo K$\alpha$ radiation (0.7107 Å) monochromatized from a graphite crystal whose diffraction vector was parallel to the diffraction vector of the sample. Three standard reflections were measured every 50 reflections. The crystal and data parameters are given in Table I. Intensity data were collected by using $\theta/2\theta$ scans. The data were reduced and the model refined by using the SHELX76[16] program package. The structures were solved using the SHELX86[16] program package. Computations were carried out on an Amdahl 5860 computer. The atomic scattering factors used were taken from ref 17. For **1** and **2**, hydrogen atoms were refined by using isotropic temperature factors. For **5**, hydrogen atoms were located, but not refined, and placed at fixed distances from bonded carbon atoms of 0.95 Å in the final difference

(6) Kneifel, H.; Bayer, E. *J. Am. Chem. Soc.* **1986**, *108*, 3075.
(7) Frank, P.; Carlson, R. M. K.; Hodgson, K. O. *Inorg. Chem.* **1988**, *27*, 118.
(8) Brand, S. G.; Hawkins, C. J.; Parry, D. L. *Inorg. Chem.* **1987**, *26*, 629.
(9) Robson, R. L.; Eady, R. R.; Richardson, T. H.; Miller, R. W.; Hawkins, M.; Postgate, J. R. *Nature (London)* **1986**, *322*, 388.
(10) Vilter, H. *Phytochemistry* **1984**, *23*, 1387.
(11) de Boer, E.; van Kooyk, Y.; Tromp, M. G. M.; Plat, H.; Wever, R. *Biochim. Biophys. Acta* **1986**, *869*, 48.
(12) Kovacs, J. A.; Holm, R. H. *Inorg. Chem.* **1987**, *26*, 702. Kovacs, J. A.; Holm, R. H. *Inorg. Chem.* **1987**, *26*, 711.
(13) Arber, J. M.; Dobson, B. R.; Eady, R. R.; Stevens, P.; Hasnain, S. S.; Garner, C. D.; Smith, B. E. *Nature (London)* **1987**, *325*, 372.
(14) de Boer, E.; Tromp, M. G. M.; Plat, H.; Krenn, G. E.; Wever, R. *Biochim. Biophys. Acta* **1986**, *872*, 104.
(15) de Boer, E.; Wever, R. *Recl.: J. R. Neth. Chem. Soc.* **1987**, *106*, 409.
(16) Sheldrick, G. M., SHELX86 and SHELX76, programs for crystal structure determinations.
(17) *International Tables for X-ray Crystallography*: Kynoch: Birmingham, England, 1974; Vol. 4.

**Table I.** Summary of Crystallographic Data for $[VO_2(HSHED)]_2$ (orange), $[VO_2(HSHED)]_2$ (yellow), and [VO(HSHED)(ACAC)]

| | $[VO_2(HSHED)]_2$ | $[VO_2(HSHED)]_2$ | [VO(HSHED)(ACAC)] |
|---|---|---|---|
| compd | **1** | **2** | **5** |
| formula | $C_{11}H_{15}N_2O_4V_1$ | $C_{11}H_{15}N_2O_4V_1$ | $C_{16}H_{22}N_2O_5V$ |
| mol wt | 290.19 | 290.19 | 372.9 |
| *a*, Å | 11.246 (3) | 10.249 (2) | 11.607 (5) |
| *b*, Å | 6.842 (2) | 10.999 (2) | 25.960 (2) |
| *c*, Å | 17.022 (5) | 10.578 (2) | 11.701 (5) |
| $\beta$, deg | 114.38 (4) | 119.16 (4) | |
| *V*, Å$^3$ | 1193.0 (6) | 1191.6 (4) | 3526 (2) |
| cryst syst | monoclinic | monoclinic | orthorhombic |
| space group | $P2_1/c$ | $P2_1/c$ | *Pbca* |
| $d_{calc}$, g/cm$^3$ | 1.616 | 1.617 | 1.410 |
| $d_{obs}$, g/cm$^3$ | 1.62 | 1.62 | 1.41 |
| *Z* | 4 | 4 | 8 |
| radiation | Mo K$\alpha$ (0.7107 Å) | Mo K$\alpha$ (0.7107 Å) | Mo K$\alpha$ (0.7107 Å) |
| abs coeff ($\mu$), cm$^{-1}$ | 8.12 | 7.80 | 5.40 |
| temp | 298 | 298 | 298 |
| cryst size, mm | 0.27 × 0.31 × 0.38 | 0.18 × 0.28 × 0.33 | 0.44 × 0.28 × 0.22 |
| scan speed, deg/min | 2.5–12 | 2.5–12 | 2.5–12 |
| scan range, deg | $0 < 2\theta < 50$ | $0 < 2\theta < 45$ | $0 < 2\theta < 45$ |
| unique data | 2114 | 1569 | 2317 |
| no. of obs data ($I > 3\sigma(I)$) | 1729 | 1265 | 1485 |
| largest nonsolv residual, e/Å$^3$ | 0.36 | 0.22 | 0.32 |
| *R* | 0.027 | 0.029 | 0.051 |
| $R_w$ | 0.027 | 0.029 | 0.040 |
| GOF | 0.67 | 0.85 | 2.14 |

**Table II.** Fractional Atomic Coordinates for $[VO_2(SHED)]_2$ (**1**)

| atom | *x* | *y* | *z* | $U$,[a] Å$^2$ |
|---|---|---|---|---|
| V1 | 0.9278 (1) | 0.9275 (1) | 0.1020 (1) | 0.021 |
| O2 | 1.0754 (2) | 0.9136 (2) | 0.0390 (2) | 0.024 |
| O3 | 0.9236 (2) | 0.8329 (2) | 0.2179 (2) | 0.029 |
| O4 | 0.8252 (2) | 0.8437 (2) | −0.0231 (2) | 0.027 |
| O5 | 1.2608 (3) | 0.9310 (3) | 0.2293 (3) | 0.057 |
| N6 | 0.7461 (3) | 1.0159 (3) | 0.1387 (2) | 0.023 |
| N7 | 0.9881 (3) | 1.0710 (3) | 0.2370 (3) | 0.024 |
| C8 | 0.7053 (3) | 0.7987 (3) | −0.0146 (3) | 0.024 |
| C9 | 0.6716 (4) | 0.6953 (3) | −0.0861 (3) | 0.031 |
| C10 | 0.5485 (4) | 0.6451 (4) | −0.0791 (3) | 0.037 |
| C11 | 0.4559 (4) | 0.6959 (4) | −0.0022 (4) | 0.037 |
| C12 | 0.4862 (4) | 0.7996 (4) | 0.0647 (4) | 0.033 |
| C13 | 0.6101 (3) | 0.8529 (3) | 0.0596 (3) | 0.024 |
| C14 | 0.6339 (4) | 0.9677 (3) | 0.1223 (3) | 0.025 |
| C15 | 0.7614 (4) | 1.1342 (4) | 0.2004 (4) | 0.030 |
| C16 | 0.8699 (4) | 1.1196 (4) | 0.2983 (4) | 0.030 |
| C17 | 1.0877 (4) | 1.0392 (4) | 0.3384 (3) | 0.032 |
| C18 | 1.2267 (4) | 1.0349 (4) | 0.2990 (4) | 0.037 |

[a] $U_{eq} = {}^1/_3\Sigma_i\Sigma_j U_{ij} a_i^* a_j^* \vec{a}_i \cdot \vec{a}_j$.

**Table III.** Fractional Atomic Coordinates for $[VO_2(SHED)]_2$ (**2**)

| atom | *x* | *y* | *z* | $U$,[a] Å$^2$ |
|---|---|---|---|---|
| V1 | 0.8437 (0) | 0.0155 (0) | 0.4728 (0) | 0.022 |
| O1 | 0.9699 (1) | 0.1541 (2) | 0.5363 (1) | 0.027 |
| O2 | 0.7151 (2) | 0.0964 (2) | 0.4808 (1) | 0.035 |
| O3 | 0.8200 (2) | 0.1119 (2) | 0.3621 (1) | 0.029 |
| O4 | 0.9258 (2) | −0.1246 (3) | 0.8005 (1) | 0.042 |
| N1 | 0.7640 (2) | −0.2496 (3) | 0.4045 (1) | 0.023 |
| N2 | 0.8830 (2) | −0.1970 (3) | 0.5747 (1) | 0.024 |
| C1 | 0.7239 (2) | 0.0770 (3) | 0.2847 (1) | 0.027 |
| C2 | 0.6953 (3) | 0.2189 (4) | 0.2201 (2) | 0.038 |
| C3 | 0.6033 (3) | 0.1825 (5) | 0.1376 (2) | 0.045 |
| C4 | 0.5373 (2) | 0.0073 (5) | 0.1175 (2) | 0.044 |
| C5 | 0.5623 (2) | −0.1340 (4) | 0.1791 (1) | 0.037 |
| C6 | 0.6557 (2) | −0.1025 (4) | 0.2643 (1) | 0.028 |
| C7 | 0.6870 (2) | −0.2619 (3) | 0.3242 (1) | 0.028 |
| C8 | 0.8011 (2) | −0.4284 (3) | 0.4561 (1) | 0.027 |
| C9 | 0.8061 (3) | −0.3793 (3) | 0.5435 (2) | 0.030 |
| C10 | 0.8661 (2) | −0.1111 (3) | 0.6498 (1) | 0.030 |
| C11 | 0.9341 (3) | −0.2287 (4) | 0.7308 (2) | 0.036 |

[a] $U_{eq} = {}^1/_3\Sigma_i\Sigma_j U_{ij} a_i^* a_j^* \vec{a}_i \cdot \vec{a}_j$.

map. Unique data and final *R* indices are reported in Table I. Fractional atomic coordinates for **1**, **2**, and **5** are given in Tables II–IV, respectively. Selected bond distances and angles for these compounds are provided in Table V.

**Table IV.** Fractional Atomic Coordinates for [VO(SHED)(ACAC)] (**5**)

| atom | *x* | *y* | *z* | $U$,[a] Å$^2$ |
|---|---|---|---|---|
| V1 | 0.0231 (1) | 0.5957 (0) | 0.1088 (1) | 0.034 |
| O1 | 0.0737 (3) | 0.5449 (2) | 0.1671 (4) | 0.038 |
| O2 | 0.1406 (4) | 0.6102 (2) | −0.0085 (4) | 0.042 |
| O3 | −0.1317 (6) | 0.6229 (3) | 0.4323 (5) | 0.076 |
| O4 | 0.0946 (4) | 0.6462 (2) | 0.2152 (4) | 0.044 |
| O5 | −0.0653 (4) | 0.6625 (2) | 0.0449 (4) | 0.041 |
| N1 | −0.0746 (4) | 0.5613 (2) | −0.0162 (5) | 0.033 |
| N2 | −0.1403 (5) | 0.5874 (2) | 0.2013 (5) | 0.035 |
| C1 | 0.1288 (6) | 0.6127 (2) | −0.1205 (6) | 0.038 |
| C2 | 0.2161 (7) | 0.6358 (3) | −0.1849 (7) | 0.047 |
| C3 | 0.2076 (8) | 0.6404 (3) | −0.3027 (8) | 0.056 |
| C4 | 0.1118 (9) | 0.6218 (4) | −0.3590 (7) | 0.058 |
| C5 | 0.0268 (8) | 0.5983 (3) | −0.2986 (6) | 0.053 |
| C6 | 0.0332 (7) | 0.5928 (3) | −0.1793 (5) | 0.038 |
| C7 | −0.0618 (6) | 0.5667 (3) | −0.1253 (6) | 0.037 |
| C8 | −0.1776 (6) | 0.5360 (3) | 0.0294 (7) | 0.041 |
| C9 | −0.2287 (6) | 0.5726 (3) | 0.1158 (7) | 0.041 |
| C10 | −0.1406 (7) | 0.5520 (3) | 0.3004 (7) | 0.047 |
| C11 | −0.0834 (8) | 0.5769 (4) | 0.4025 (8) | 0.064 |
| C12 | −0.0390 (7) | 0.7092 (3) | 0.0577 (6) | 0.044 |
| C13 | 0.0410 (8) | 0.7264 (3) | 0.1386 (7) | 0.059 |
| C14 | 0.1002 (7) | 0.6952 (3) | 0.2129 (6) | 0.050 |
| C15 | −0.0982 (8) | 0.7469 (4) | −0.0188 (8) | 0.071 |
| C16 | 0.1791 (10) | 0.7186 (4) | 0.3003 (9) | 0.081 |

[a] $U_{eq} = {}^1/_3\Sigma_i\Sigma_j U_{ij} a_i^* a_j^* \vec{a}_i \cdot \vec{a}_j$.

**Electrochemical Measurements.** Electrochemical measurements were completed at 23 ± 2 °C by using a BAS-100 electrochemical analyzer. Cyclic voltammetry was performed on a three-electrode system composed of platinum-bead, platinum-wire, and saturated calomel (SCE, within a Lugin probe) electrodes as the working, auxiliary, and reference electrodes, respectively. (TBA)$PF_6$ was used as the supporting electrolyte at 0.1 M concentration. All potentials are referenced versus the ferrocene/ferrocenium couple employed as an external reference.

**Spectroscopic and Magnetic Measurements.** UV/vis spectra were recorded on a Perkin-Elmer Lambda 9 UV/vis/near-IR spectrophotometer equipped with a Perkin-Elmer 3600 data station. Infrared spectra were recorded on a Nicolet 60 SX Fourier transform spectrometer with samples prepared as KBr pellets. Solution EPR spectra were recorded on a Bruker ER200 E-SRC spectrometer equipped with a liquid-nitrogen Dewar and a Varian variable-temperature controller. DPPH ($g$ = 2.0037) was used as an external standard. Room-temperature solid-state magnetic moments were calculated from data obtained on a Johnson Matthey magnetic susceptibility balance. Solution susceptibilities were calculated from data obtained with a Bruker 360-MHz NMR spectrometer by using the Evans method.[18]

**Table V.** Selected Bond Distances (Å) and Angles (deg) for $[VO_2(HSHED)]_2$ (**1**), $[VO_2(HSHED)]_2$ (**2**), and [VO(HSHED)(ACAC)]

| $[VO_2(HSHED)]_2$ (**2**) | | $[VO_2(HSHED)]_2$ (**1**) | | [VO(HSHED)(ACAC)] (**5**) | |
|---|---|---|---|---|---|
| V1–O1 | 1.678 (2) | V1–O1 | 1.682 (2) | V1–O1 | 1.596 (4) |
| V1–O2 | 1.605 (2) | V1–O2 | 1.610 (2) | V1–O2 | 1.972 (4) |
| V1–O3 | 1.909 (2) | V1–O3 | 1.897 (2) | V1–O4 | 1.989 (4) |
| V1–N1 | 2.141 (3) | V1–N1 | 2.149 (3) | V1–O5 | 2.149 (4) |
| V1–N2 | 2.164 (3) | V1–N2 | 2.202 (3) | V1–N1 | 2.054 (5) |
| V1–O1′ | 2.455 (2) | V1–O1′ | 2.298 (2) | V1–N2 | 2.194 (5) |
| V1–V1′ | 3.251 (1) | V1–V1′ | 3.103 (1) | | |
| V1–OOP[a] | 0.357 Å | V1–OOP[a] | 0.294 Å | | |
| O1–V1–O2 | 107.6 (1) | O1–V1–O2 | 107.0 (1) | O1–V1–O2 | 101.6 (2) |
| O1–V1–O3 | 100.2 (1) | O1–V1–O3 | 99.4 (1) | O1–V1–O4 | 97.1 (2) |
| O2–V1–O3 | 101.6 (1) | O2–V1–O3 | 100.8 (1) | O2–V1–O4 | 91.2 (2) |
| O1–V1–N1 | 151.8 (1) | O1–V1–N1 | 155.6 (1) | O1–V1–O5 | 172.2 (2) |
| O2–V1–N1 | 98.5 (1) | O2–V1–N1 | 96.2 (1) | O2–V1–O5 | 86.2 (2) |
| O3–V1–N1 | 84.3 (1) | O3–V1–N1 | 83.4 (1) | O4–V1–O5 | 83.4 (2) |
| O1–V1–N2 | 91.5 (1) | O1–V1–N2 | 95.0 (1) | O1–V1–N1 | 98.5 (2) |
| O2–V1–N2 | 93.3 (1) | O2–V1–N2 | 89.1 (1) | O2–V1–N1 | 88.2 (2) |
| O3–V1–N2 | 157.3 (1) | O3–V1–N2 | 159.3 (1) | O4–V1–N1 | 164.1 (2) |
| N1–V1–N2 | 76.5 (1) | N1–V1–N2 | 77.5 (1) | O5–V1–N1 | 80.7 (2) |
| O1–V1–O1′ | 77.9 (1) | O1–V1–O1′ | 78.7 (1) | O1–V1–N2 | 91.5 (2) |
| O2–V1–O1′ | 171.9 (1) | O2–V1–O1′ | 170.4 (1) | O2–V1–N2 | 163.8 (2) |
| O3–V1–O1′ | 82.9 (1) | O3–V1–O1′ | 85.6 (1) | O4–V1–N2 | 96.7 (2) |
| N1–V1–O1′ | 75.1 (1) | N1–V1–O1′ | 77.4 (1) | O5–V1–N2 | 80.7 (2) |
| N2–V1–O1′ | 80.5 (1) | N2–V1–O1′ | 82.6 (1) | N1–V1–N2 | 80.3 (2) |
| V1–O1–V1′ | 102.1 (1) | V1–O1–V1′ | 101.3 (1) | | |
| O1–V1–O1′ | 77.9 (1) | O1–V1–O1′ | 78.7 (1) | | |

[a] OOP = out-of-plane distance for plane defined as O1–O3–N1–N2.

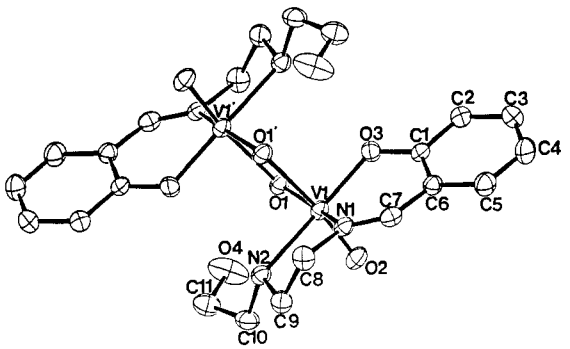


**Figure 1.** ORTEP diagram of $[VO_2(HSHED)]_2$ (**1**) with thermal ellipsoids at 30% probability. Selected bond lengths and angles are given in Table V.

## Results and Discussion

**Description of $VO_2$(HSHED) Structures.** Reaction of vanadyl sulfate or $VO(ACAC)_2$ with $H_2SHED$ in methanolic solution yields directly either of the weakly associated dimers **1** or **2**. These compounds represent the first examples of two pervanadyl units forming a bis($\mu$-oxo)-bridged V(V) Schiff base dimer. An ORTEP diagram of **1** is given in Figure 1, and selected bond lengths and angles for both **1** and **2** are presented in Table V. The structure of **1** demonstrates that each V(V) ion is six-coordinate with two distinct oxo groups being apparent. The first of these (V1–O2) is a typical V=O distance of 1.610 Å. The second oxo group is involved in the bridge between V1 and V1′. It is strongly coordinated to V1 (V1–O1, 1.682 Å) and is weakly associated with V1′ (V1′–O1, 2.298 Å). The remaining three coordination sites are occupied by the phenolate oxygen (V1–O3, 1.897 Å), imine nitrogen (V1–N1, 2.149 Å), and amine nitrogen (V1–N2, 2.202 Å) atoms of the ligand with the hydroxyl group remaining uncoordinated. Thus, the coordination sphere of the vanadium ions are composed of six unique heteroatom types: vanadyl oxo atoms, two bridging oxo atoms at short and long distances, a phenolate oxygen atom, and imine and amine nitrogen atoms. The polyhedron that is described resembles two edge shared octahedra that are very significantly distorted. The O1–V1–O2 angle is 107.0°, a value that is close to that observed for $VO_2$EDTA,[19] $VO_2(8\text{-}Q)_2$,[20] and many other *cis*-$VO_2^+$ (pervanadyl) units.[21] Angles described by trans substituents are far from 180°, ranging from 155.6° to 170.4°. The two $VO_2$HSHED units are related by an inversion center with a vanadium–vanadium distance of 3.103 Å.

**Table VI.** V=O Stretching Frequencies for V(IV) and V(V) Complexes

| complex | $\nu$(V=O), cm$^{-1}$ | medium | coordn geometry[a] | ref |
|---|---|---|---|---|
| $NH_4$[VO(EHPG)] | 948 | KBr | six-coord | 28 |
| Na[VO(EHGS)] | 952 | KBr | six-coord | 28 |
| VO(SALEN) | 981 | KBr | square pyramidal | 28 |
| VO(SALEN) | 953 | DMSO | (six-coord) | 28 |
| **5** | 953 | KBr | six-coord | |
| **6** | 928 | KBr | (six-coord) | |
| **1** | 929 | KBr | six-coord | |
| **2** | 939 | KBr | weakly six-coord | |

[a] Geometry in parentheses is that suggested by IR data; others were determined crystallographically.

The yellow solid, dimer **2**, is analogous to **1** except that the oxo bridge is much weaker. A comparison of the metal–heteroatom distances between **1** and **2** shows that the first coordination spheres are nearly identical. The primary difference is in the V1–O1′ distances (2.298 Å in **1**; 2.455 Å in **2**). This long interaction leads to a significant lengthening of the V1–V1′ distance in **2** (3.103 Å in **1**; 3.251 Å in **2**). Both materials are related to square-pyramidal parent compounds with weak ligation trans to the strong V=O bond. The V(V) is displaced out of the best least-squares plane defined by O1, O3, N1, and N2 by 0.294 Å in **1** and by 0.357 Å in **2**. The IR spectra of the two materials are similar, but not identical. Compound **2** shows V=O stretches at 969 and 939 cm$^{-1}$ in agreement with previously described complexes containing the pervanadyl moiety. However, assignment of the V=O stretches in the more strongly associated dimeric material is more difficult. We observe that there are five bands in the region 900–1000 cm$^{-1}$ for this complex. The strongest of these peaks is centered at 929 cm$^{-1}$. The structural data are consistent with the infrared spectra as the more weakly associated compound

(18) Bartle, K. D.; Dale, B. J.; Jones, D. W.; Maricic, J. *J. Magn. Reson.* **1973**, *12*, 286. Evans, D. F. *J. Chem. Soc.* **1959**, 2003.

(19) Scheidt, W. R.; Collins, D. M.; Hoard, J. L. *J. Am. Chem. Soc.* **1971**, *93*, 3873. Scheidt, W. R.; Countryman, R.; Hoard, J. L. *J. Am. Chem. Soc.* **1971**, *93*, 3878.

(20) Giacomelli, A.; Floriani, C.; de Souza Duarte, A. O.; Chiesi-Villa, A.; Guastini, C. *Inorg. Chem.* **1982**, *27*, 3310.

(21) Scheidt, W. R. *Inorg. Chem.* **1973**, *12*, 1758.

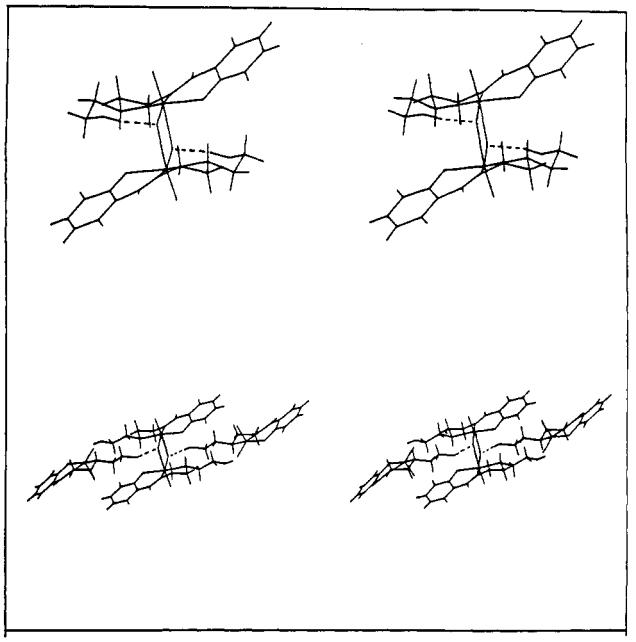

**Figure 2.** Comparison of the hydrogen bonding seen in **1** and **2**. An intramolecular hydrogen bond is observed in **1**, while an intermolecular hydrogen-bonded chain network is seen in crystals of **2**.

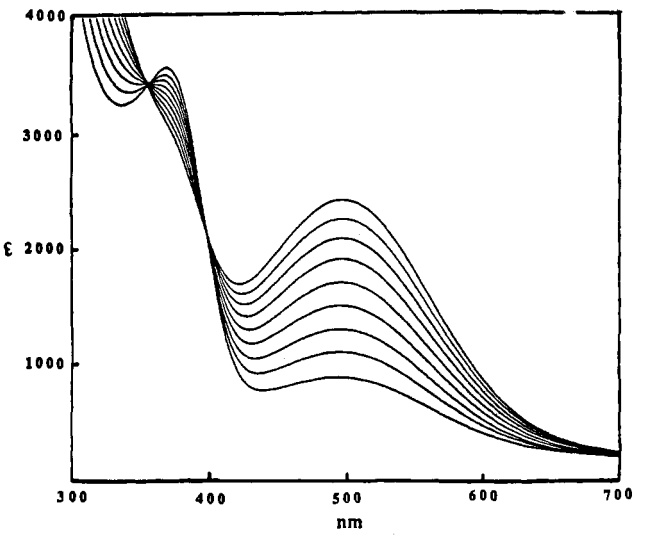


**Figure 3.** Titration of **2** with 0.187 M HCl in acetonitrile. Isosbestic points are observed at 354 and 398 nm for the equilibrium between **2** and **3**. The $VOOH(HSHED)^+$ ion has a strong absorbance at 496 nm. The titration is shown through 0.7 equiv of added $H^+$. Above this point, small amounts of **4** are generated. This $VO(HSHED)^{2+}$ ion is very unstable, decomposing in less than a minute.

exhibits the higher energy V=O stretch (Table VI).

Compounds **1** and **2** are obviously related through a very soft potential surface. In **1**, the uncoordinated hydroxyl forms an intramolecular hydrogen bond to the bridging oxo group that originates from the same monomeric unit. A stick figure representation of this hydrogen bonding is shown as Figure 2. In contrast, an intermolecular hydrogen bond between the hydroxyl group of one dimer to the bridging oxo atom of another unit is present in **2**. This generates a hydrogen-bonded chain structure running through the crystal. The observed structural differences between **1** and **2** probably reflect both crystal packing forces and a very short hydroxyl oxygen–imine carbon contact (2.9 Å), which is a result of the hydrogen bonding in **2**. The driving force for the formation of **1** and **2** is apparent when one considers the vacant coordination site of a monomeric material and the lack of other suitable heteroatom donors in the crystals.

**Comparison of Structures to Those of Related Vanadium Complexes.** Although a common structural motif in fused polyvanadates, the $V_2O_4$ core is rarely observed in discrete coordination compounds. Wieghardt[22] has reported the structure of $V_2O_2(\mu\text{-}OH)_2([9]aneN_3)_2]Br_2$, a bis($\mu$-hydroxy)-bridged vanadium(IV) dimer **7**. The core of this molecule is similar to that reported herein for the bis($\mu$-oxo)-bridged vanadium(V) dimer $[VO_2(HSHED)]_2$. The V(IV)–V(IV) distance is 3.033 Å as compared to 3.103 Å for **1**. One expects the acute O1–V1–O1′ angle (78.7°) and the obtuse V1–O1–V1′ angle (101.3°) since metal–metal bonding is not possible in **1**. This is also observed for **7**, which is weakly antiferromagnetically coupled, but is in stark contrast to the metal–metal singly bonded, $d^1$–$d^1$ $Mo_2O_2(\mu\text{-}OH)_2([9]aneN_3)_2]$,[23] which has an obtuse O1–Mo1–O1′ angle and an acute Mo1–O1–Mo1′ angle. One interesting distinction between **1** and **7** is the V1–O1 and V1–O1′ bond distances. A very asymmetric bridge is seen for **1** with V1–O1 at 1.682 Å and V1–O1′ at 2.298 Å. This illustrates that the V1–O1 bond is essentially a V=O bond (as compared with V1–O2 at 1.610 Å). The core of **7**, however, is much more symmetrical (V1–O1, 1.956 Å; V1–O1′, 1.969 Å) with distances consistent with hydroxide ligation.

These bridging interactions may be a consequence of the coordination geometry enforced by the ligands. The bicyclic chelate rings formed by the phenolate, imine, and amine atoms of $HSHED^-$ are oriented in a meridional configuration while the cyclononane ([9]aneN$_3$) forms a facial tridentate chelate. The V1–O1′ bridge is trans to the strong V1–O2 double bond in the meridional complex (**1**). In the case of the V(IV) complex (**7**), which has a facial geometry, the ligand nitrogen atoms are positioned trans to the vanadyl bond at long distances (2.303 Å). Thus, both compounds show strong trans influences; however, in the V(V) complexes of $HSHED^-$, the trans effect serves to weaken significantly the metal–bridging atom bonds.

Other examples of oxygen bridges have been reported, but these structures are easily distinguished from that of **1** or **2**. Stomberg has reported $\mu$-oxo, diperoxovanadate dimers,[24-26] and linear $\mu$-oxo bridges have been observed in V(IV)/V(V) mixed-valence compounds[27-30] with the $V_2O_3$ core. In the latter case, the nearly linear and closely symmetrical single oxo atom bridges in the mixed-valence dimers lead to large V–V separations (>3.6 Å). The dimeric pentagonal-bipyramidal peroxovanadates often contain a strong $\mu$-oxo bridge and weaker peroxo donation to the second vanadium atom. Alternatively, oxo-bridged chains are observed for $(NH_4)_2[VFO(O_2)_2]$.[26]

**Solution Chemistry of V(V) Complexes.** Both **1** and **2** are very robust in acetonitrile. The proton NMR and UV/vis spectra demonstrate that the compounds are indistinguishable in solution and, most likely, convert to the same solvated, monomeric material. Addition of anhydrous 0.187 M HCl in acetonitrile to a solution of **2** yields the progressive generation of a red material ($\lambda$ = 496 nm; $\epsilon$ = 1300 $M^{-1}$) as illustrated in Figure 3. The isosbestic points at 398 and 354 nm demonstrate the equilibrium between **2** and **3**. After the addition of 0.8 equiv, a second reaction becomes apparent. The solution turns violet and rapidly bleaches back to the initial red color. If an excess of acid (2 equiv) is added in one aliquot, the solution turns deep blue (**4**, $\lambda$ = 596 nm) and then bleaches to a very pale red-violet in less than a minute. We have not determined precisely the extinction coefficient of **4** due to its instability; however, we conservatively estimate it to be greater than or equal to 5000 $M^{-1}$. Identical chemistry is observed if **1**

(22) Wieghardt, K.; Bossek, U.; Volckmar, K.; Swirdoff, W.; Weiss, J. *Inorg. Chem.* **1984**, *23*, 1387.
(23) Wieghardt, K.; Hahn, M.; Swirdoff, W.; Weiss, J. *Angew. Chem., Int. Ed. Engl.* **1983**, *22*, 491.
(24) Stomberg, R.; Olson, S.; Svenson, I.-B. *Acta Chem. Scand.* **1984**, *A38*, 653.
(25) Szentivanyi, H.; Stomberg, R. *Acta Chem. Scand.* **1983**, *A37*, 553.
(26) Stomberg, R.; Olson, S. *Acta Chem. Scand.* **1984**, *A38*, 801.
(27) Launay, J.-P.; Jeannin, Y.; Daoudi, M. *Inorg. Chem.* **1985**, *24*, 1052.
(28) Babonneau, F.; Sanchez, C.; Livage, J.; Launay, J. P.; Daoudi, M.; Jeannin, Y. *Nouv. J. Chim.* **1982**, *6*, 353.
(29) Nishizawa, M.; Hirotsu, K.; Ooi, S.; Saito, K. *J. Chem. Soc., Chem. Commun.* **1979**, 707.
(30) Kojima, A.; Okazaki, K.; Ooi, S.; Saito, K. *Inorg. Chem.* **1983**, *22*, 1168.

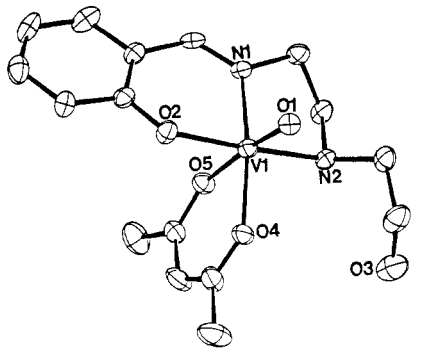


**Figure 4.** ORTEP diagram of [VO(HSHED)(ACAC)] with thermal ellipsoids at 30% probability. Selected bond lengths and angles are given in Table V.

is used in these titrations. When **1** and **2** are acidified in DMF or DMSO, a rust-pink solution is generated that does not turn blue upon further addition of acid. On the basis of the proton stoichiometries of these reactions and the previously described chemistry of $VO(SALEN)^+$,[31,32] $VO(EHPG)^-$,[33,34] VO(EHGS),[33,34] and $(8\text{-Q})_2VO(OH)$,[20] we assign **3** as a $V^VO(OH)HSHED^+$ complex and the deep blue, highly unstable material **4** as the monooxovanadium(V)–HSHED complex $VO(HSHED)^{2+}$.

The strong absorptivity of the V(V) complexes (**3** and **4**) must be due to a ligand to metal charge-transfer excitation. Intense charge-transfer spectra have been observed for the monooxovanadium(V) phenolates[31-34] VO(EHPG), VO(EHGS), and $VO(SALEN)^+$. In addition, weaker transitions are observed at higher energy for previously characterized V(V)–oxo–hydroxo–phenolate-based species. The results presented herein are in agreement with these observations. Thus, it appears that intense charge-transfer spectra in the 570–610-nm range are a hallmark of $VO^{3+}$ phenolates.

Neither of the $[VO_2(HSHED)]_2$ complexes gives clean electrochemical behavior in any of the solvents in which they were examined. Three ill-defined waves at −1.2, −1.5, and −1.8 V were observed for both materials in acetonitrile. Rapid passivization of the electrode, generating a single very broad wave, prohibited detailed electrochemical characterization of these reductions. Titration of either **1** or **2** in acetonitrile with anhydrous HCl in acetonitrile provided additional evidence for the formation of VO(OH)HSHED (**4**). Two waves developed at +190 and −660 mV as hydrogen ion was added. We assign the wave at +190 mV as the V(V)/V(IV) reduction of the red compound **4**. The wave at −660 mV arises from excess $H^+$, which is introduced into the cell during the titration. The red solution decomposed very slowly until greater than 3 equiv of acid was added to the electrochemical cell. At this point, the solution turned violet and eventually, on addition of more acid, deep blue. Unfortunately, the rapid decomposition of the blue compound precluded a study of its electrochemical behavior.

**Chemistry of the V(IV) Complexes.** Oxovanadium(IV) complexes of $HSHED^-$ can also be prepared, but methanol and DMF solutions are air sensitive, ultimately resulting in the formation of the dimers **1** and **2**. When $VO(ACAC)_2$ was reacted in degassed methanol, deep red crystals of **5**, which were suitable for X-ray diffraction studies, were isolated and indicated that the oxovanadium(IV)–HSHED–ACAC complex illustrated in Figure 4 had been isolated. As was observed in the structure of the vanadium(V) dimer, the HSHED ligand acts as a tridentate chelating agent, using phenolate, imine, and amine heteroatom donors in a meridional orientation. The hydroxyl group remains uncoordinated. The V=O distance is typical of the vanadyl unit (1.596 Å). Six-coordination is satisfied by the coordinated ACAC moiety. As expected, the oxygen trans to the V=O group is significantly elongated (2.149 Å) relative to the ACAC oxygen in the equatorial plane (1.989 Å). Unlike compounds **1**–**4** described above, **5** is paramagnetic ($\mu_{eff}$ = 1.67 $\mu_B$) and at room temperature exhibits an eight-line EPR spectrum in DMF. The 77 K spectrum provides $g_\parallel$ (1.95; $A_\parallel = 153 \times 10^{-4}$ cm$^{-1}$) and $g_\perp$ (1.98; $A_\perp = 60 \times 10^{-4}$ cm$^{-1}$). The EPR spectral parameters of the vanadium bromoperoxidase from *A. nodosum* have recently been measured[35] in aqueous, citrate-buffered solution. These values are presented in Table VII for direct comparison to those values for **5** and **6**. As can be seen, compound **6** is intermediate between the high and low pH forms of the enzyme.

**Table VII.** Physical Parameters for Vanadium HSHED Compounds

| complex | UV/vis[a] $\lambda_{max}$, nm ($\epsilon$, M$^{-1}$) | $\mu_{eff}$, $\mu_B$ | EPR |
|---|---|---|---|
| **1** | 371 (3400) | diamag[b,c] | |
| **2** | 371 (3400) | diamag[b,c] | |
| **3** | 496 (1300) | diamag[d] | |
| **4** | 596 (≈5000) | diamag[d] | |
| **5** | 353 (3900) | 1.67[c] | $g_{iso}$[e] = 1.971 (91)[g] |
| | 372 (4010) | | $g_\perp$[f] = 1.982 (60)[g] |
| | 553 (87) | | $g_\parallel$[f] = 1.950 (153)[g] |
| | 780 (37) | | |
| **6** | 375 (3800)[e] | 1.68[d] | $g_{iso}$[e] = 1.968 (97)[g] |
| | 564 (93)[e] | | $g_\perp$[f,g] = 1.979 (64)[g] |
| | | | $g_\parallel$[f,g] = 1.947 (162)[g] |
| vanadium(V) bromoperoxidase[35] | | high pH | $g_{iso}$[e] = 1.969 (87)[g] |
| | | | $g_\perp$[f,g] = 1.979 (50)[g] |
| | | | $g_\parallel$[f,g] = 1.948 (160)[g] |
| | | low pH | $g_{iso}$[e] = 1.970 (93)[g] |
| | | | $g_\perp$[f,g] = 1.980 (55)[g] |
| | | | $g_\parallel$[f,g] = 1.950 (168)[g] |

[a] Determined in acetonitrile. [b] Determined in the solid state. [c] Determined in DMSO. [d] Precise determination of the magnetic susceptibility is difficult due to the short half-life of the complex; however, there is no evidence for a paramagnet being generated by the acidification process. Solutions of the blue compound that are rapidly frozen and for which EPR spectra have been run give no indication of an EPR signal. [e] Calculated from $g_{iso} = (g_\parallel + 2g_\perp)/3$; $A_{iso} = (A_\parallel + 2A_\perp)/3$. [f] Measured at 77 K. [g] $A_{iso}$, $A_\perp$, and $A_\parallel$ are reported in units of $10^{-4}$ cm$^{-1}$ and are given in parentheses.

A deep green solution results if 1 equiv of base is added to a degassed methanol solution containing **5**. This solution is even more air sensitive than is **5**; however, when the green solid (**6**) is recovered, it is stable in air. The compound is paramagnetic and shows an eight-line EPR spectrum, indicating that it too is a vanadium(IV) compound. An oxo stretch at 921 cm$^{-1}$ is observed and IR bands associated with the ACAC ligand in the spectrum of **5** are no longer apparent. Furthermore, the intensity in the 3400-cm$^{-1}$ region is dramatically decreased. The green material is a nonelectrolyte in methanol. These observations, when taken together, suggest that **6** is VO(SHED), in which the alkoxide oxygen atom is now coordinated to the vanadium and the acetonylacetonate ligand has been displaced. Elemental analysis of **6** is also consistent with this formulation.

Bonadies and Carrano[34] have shown that the coordination number of oxovanadium(IV) Schiff base complexes can be assigned based on the V=O stretch. These data are presented in Table VI. Values of ≈950 cm$^{-1}$ are indicative of six coordination in a distorted octahedral geometry while values of ≈980 cm$^{-1}$ are associated with five-coordination (square pyramidal). Compound **5**, a crystallographically characterized member of this series, follows this trend nicely (953 cm$^{-1}$). The green VO(SHED) has a very low-energy V=O stretch (921 cm$^{-1}$), indicating that it is, most likely, six-coordinate in the solid state. This coordination position is probably occupied by solvent.

In contrast to the V(V) phenolates discussed above, $VO^{2+}$ compounds such as VO(SALEN) have visible transitions that are

(31) Bonadies, J. A.; Pecoraro, V. L.; Carrano, C. J. *J. Chem. Soc., Chem. Commun.* **1986**, 1218.
(32) Bonadies, J. A.; Butler, W. M.; Pecoraro, V. L.; Carrano, C. J. *Inorg. Chem.* **1987**, *26*, 1218.
(33) Pecoraro, V. L.; Bonadies, J. A.; Marese, C. A.; Carrano, C. J. *J. Am. Chem. Soc.* **1985**, *107*, 1651.
(34) Bonadies, J. A.; Carrano, C. J. *J. Am. Chem. Soc.* **1986**, *108*, 4088.
(35) de Boer, E.; Boon, K.; Wever, R. *Biochemistry* **1988**, *27*, 1629.

**Table VIII.** Electrochemistry of Vanadium SHED Complexes[a]

| complex | $E_c$[b] | $E_a$[b] | $\Delta E$ | $i_c$[c] | $i_a$[c] | $i_c/i_a$ |
|---|---|---|---|---|---|---|
| **1** or **2** | −1800 | | | 1.2 | | |
| | −1500 | | | 2.4 | | |
| | −1200 | | | 0.7 | | |
| **3** | | +193[e] | | | 1.2 | |
| **5** | +482[e] | +551[e] | 69 | 4.1 | 6.3 | 0.65 |
| | +287 | | | 0.3 | | |
| | +500[f] | +580[f] | 80 | 3.0 | 3.8 | 0.79 |
| | +311[f] | | | 0.06 | | |
| | | +1143[g] | | | 0.16 | |
| | +477[g] | +543[g] | 66 | 0.5 | 1.6 | 0.31 |
| | +116[g] | +219[g] | 103 | 0.53 | 0.24 | 2.2 |
| | +449[h] | +539[h] | 90 | 2.7 | 8.6 | 0.31 |
| | +50[h] | | | 4.1 | | |
| **6** | | +939[g] | | 0.4 | | |
| | +108[g] | +171[g] | 63 | 0.5 | 1.3 | 0.38 |
| | +50[h] | +149[h] | 90 | 2.6 | 3.4 | 0.76 |

[a] Electrode configuration and conditions given in text. [b] In millivolts versus SCE referenced to the ferrocene/ferrocenium couple. [c] Current × $10^{-6}$. [d] DMSO. [e] Acetonitrile. [f] Methylene chloride. [g] DMF. [h] Methanol.

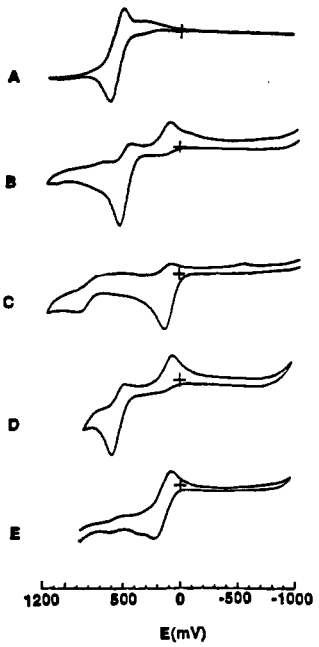


**Figure 5.** Cyclic voltammograms of **5** and **6** in various solvents: (A) **5** in methylene chloride; (B) **5** in DMF; (C) **6** in DMF; (D) **5** in methanol; (E) **6** in methanol. Potentials are referenced against the standard calomel electrode by using the ferrocene/ferrocenium couple as an external reference. Scan rate = 50 mV/s.

predominantly d–d in character.[34] Such is the case for VO(HSHED)(ACAC) and VO(SHED) as illustrated by the spectral characteristics presented in Table VII. Three d–d transitions are predicted[34] for these complexes, decreasing in energy in the order $b_2 \rightarrow a_1 > b_2 \rightarrow b_1 > b_2 \rightarrow e$. The highest energy d–d band is obscured by the strong absorbance in the UV region for both complexes. The transition $b_2 \rightarrow b_1$, which yields $10Dq$, is seen at 553 nm (18 100 $cm^{-1}$) and 564 nm (17 700 $cm^{-1}$) for **5** and **6**, respectively. The lowest energy band is observed only for VO(SHED)(ACAC) at 780 nm.

The electrochemical behavior of **5** and **6** in various solvents is illustrated in Figure 5 and tabulated in Table VIII. Figure 5a shows that the cyclic voltammogram of **5** in methylene chloride exhibits a nearly reversible one-electron oxidation at +580 mV. This is consistent with the solution chemistry of **5** in methylene chloride and also acetonitrile (Table VII), since VO(HSHED)(ACAC) is not air sensitive in these solvents. The voltammograms of **5** in DMF (Figure 5b) and methanol (Figure 5d) one again show an oxidative wave in the +500-mV region. However, there are additional, irreversible oxidations at $p_a$ = +219 mV in DMF and $p_a \approx$ +150 mV in methanol that were not observed in the acetonitrile voltammetry. In both of these solvents, solutions of **5** will convert to **1** if left standing in air for a few days (the reaction proceeds slightly faster in methanol than in DMF). Therefore, we believe that it is the species with a potential in the +50- to +250-mV range that is involved in the air oxidation process, rather than **5** itself. Related vanadium complexes[31,34] with potentials in the 0 to +150 mV range are also observed to be air sensitive. For this reason, we were interested in identifying the material that led to the generation of **1**. It seemed reasonable that the ACAC moiety would dissociate in the better donor solvents of methanol and DMF. The removal of this group as an anion generates $VO(HSHED)^+$, which one would anticipate would be more difficult to oxidize than **5**. This may account for the wave in DMF at ≈+1 V, which increases in intensity upon addition of acid and decreases with added base. However, if the loss of ACAC was associated with the deprotonation and insertion of an alkoxide oxygen into the vanadium coordination sphere, a more easily oxidized material should be produced. In fact, **6** is precisely this compound, and it does have a much shorter solution halflife in generating **1** than does **5**. To test this hypothesis, we examined the cyclic voltammetry of **6** in DMF (Figure 5c) and methanol (Figure 5e). As shown in Table VIII, the potentials for **6** in these solvents are nearly identical with those for the minor species generated in the methanol and DMF solutions of **5**. Therefore, we believe that the air sensitivity of solutions containing **5** is not a direct chemical conversion of **5** to form **1** but actually proceeds through the generation of a small amount of **6** in oxygen donor solvents.

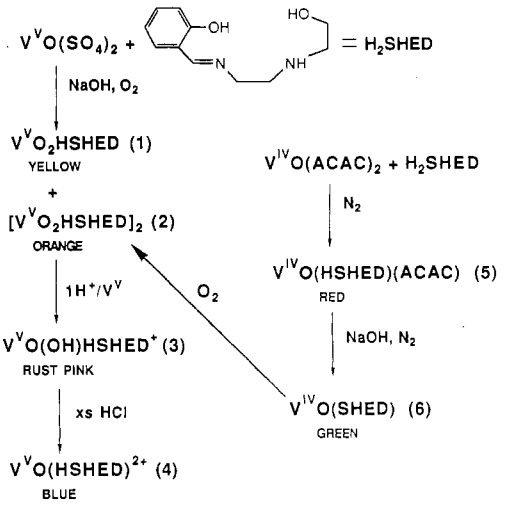


**Figure 6.** Relationship of the vanadium complexes described in the text. Dinuclear bis(μ-oxo)-$VO_2^+$ and mononuclear $VOOH^{2+}$ and $VO^{3+}$ compounds are seen in the V(V) oxidation level while vanadyl complexes with and without acetonylacetonate are isolated in the V(IV) oxidation level. The green $V^{IV}O$(SHED) is air-sensitive, generating the V(V) dimers. Methanolic and DMF solutions of VO(HSHED)(ACAC) are air-sensitive, forming the V(V) dimers by dissociation of the ACAC moiety to generate a small amount of the green V(IV) monomer. Compounds **1** and **2** can be converted to **3** by the addition of 1 equiv of $H^+$ per vanadium(V). The deep blue solutions of **4** result from the addition of excess acid. The indicated colors are for the recovered solid except for compounds **3** and **4**, which were not isolated. The colors in these cases correspond to those of an acetonitrile solution of the appropriate complex.

**Interrelation of Vanadium–SHED Complexes.** We can now summarize the interrelationship of the vanadium(IV) and vanadium(V) compounds characterized in this study by using Figure 6 as a frame of reference. The most stable complexes of $HSHED^-$ appear to be the weakly associated solid-state dimers containing the pervanadyl unit and $HSHED^-$ as a tridentate chelating agent. This material is isolated in greater than 80% yield when V(IV) salts are reacted with $H_2SHED$ in neutral or slightly basic methanol solution. One can isolate an air-stable red solid, VO(HSHED)(ACAC), if the reaction is run under nitrogen; however, when dissolved in methanol or DMF, this material slowly converts to the V(V) dimer. Electrochemical analysis indicates that this

conversion is not direct. Rather, oxidation appears to proceed through the dissociation of an ACAC moiety to give the green VO(SHED), the only isolated complex in which the ligand is tetradentate with a coordinated alkoxide. The pervanadyl dimers most likely dissociate into monomeric units when dissolved in DMF or DMSO. It is difficult to establish whether monomers are formed in acetonitrile due to the low solubility in this solvent. When anhydrous acid is added to an acetonitrile solution of **1** or **2**, the red $VO(OH)HSHED^+$ complex is formed. This compound is stable, and the acid-base chemistry is reversible, up to 0.8 equiv. Beyond this point, a deep blue monooxovanadium(V)-$HSHED^{2+}$ complex is observed, which is too unstable to be isolated.

**Potential Biological Relevance.** The vanadium bromoperoxidases are known to contain vanadium(V) in the resting oxidation level of the enzyme, and no evidence has been forwarded to suggest vanadium(IV) as a participant in catalysis. To date, every well-characterized monooxovanadium(V)[31-34] and bare vanadium(V)[36] complexes containing phenolates exhibit strong ligand to metal charge-transfer absorption spectra in the 600-nm range. Clearly such an absorbance is not present, at least in the isolated forms, in the vanadium peroxidases. This leads to the conclusion that bare vanadium(V) or monooxovanadium(V) coordinated to a phenolate is not an appropriate description for this enzyme's resting state. The following possibilities for the metal site then results: (1) tyrosine may not be a ligand to vanadium in these enzymes; (2) active-site vanadium may be in the form of the pervanadyl moiety rather than bare V(V) or $VO^{3+}$; (3) possibilities 1 and 2 both may be operable. Given the strong aqueous reactivity of bare V(V) or $VO^{3+}$, it is most likely that at least point 2 is correct.

Floriani[20] has suggested the vanadate/carboxylate analogy to understand the reactivity and structural possibilities for the pervanadyl unit. Support for this notion comes from the facile protonation of the $VO_2^+$ unit and the isolation of vanadate esters such as $VO(OC(CH_3)_3)(8\text{-}Q)_2$.[21] One possible intermediate in the enzymatic reaction is hypobromite coordinated to V(V), $VO(OBr)^{2+}$. The corresponding acyl hypobromite, RCO(OBr), is an excellent reagent for bromodecarboxylation of aliphatic or aromatic carboxylic acids in the Hunsdiecker reaction[37] and, more interestingly, can brominate directly activated aromatics in a "non-Hunsdiecker" halogenation.[38] Thus, extension of this analogy to the enzymatic system may prove fertile. The SHED complexes described herein may provide an useful entry into the reactivity of these complexes due to the open sixth coordination site. Thus, direct reaction with hydrogen peroxide to generate materials similar to those described by Stomberg[24-26] or the joint reaction of hydrogen peroxide and bromide with $[VO_2(HSHED)]_2$ may provide reactivity analogues for the enzymatic process. In addition, the $^{51}V$ NMR spectra of these and related complexes may be useful in defining the first coordination sphere ligands of the peroxidase.[39-42] The value of -529 ppm in DMSO vs $VOCl_3$ indicates that the $VO_2(HSHED)$ complex does not model well the extraordinarily large shift seen for the enzyme[40] (-1200 ppm). The NMR behavior of other analogues of these complexes is presently being explored.

**Acknowledgment.** We thank Prof. Alison Butler (UCSB) for allowing us to quote her values for the $^{51}V$ NMR spectra of the vanadium SHED complexes prior to publication. Dr. Joseph Bonadies is thanked for a very useful discussion relating to this and the EHPG work described in this paper. V.L.P. thanks the G. D. Searle Family/Chicago Community Trust for a Biomedical Research Scholar's Award (1986-1989).

**Supplementary Material Available:** Tables 9, 14, and 19, listing anisotropic thermal parameters, Tables 10, 15, and 20, listing fractional atomic positions for hydrogen atoms, Tables 11, 16, and 21, listing the complete set of bond distances, Tables 12, 17, and 22, listing the complete set of bond angles, and Figures 7, 8, and 9, providing complete numbering schemes for **1**, **2**, and **5**, respectively (15 pages); Tables 13, 18, and 23, listing observed and calculated structure factors (20 pages). Ordering information is given on any current masthead page.

(36) Cooper, S. R.; Bai Koh, Y.; Raymond, K. N. *J. Am. Chem. Soc.* **1982**, *104*, 5092.
(37) Johnson, R. G.; Ingham, R. K. *Chem. Rev.* **1957**, 219.
(38) Dauben, W. G.; Tilles, H. *J. Am. Chem. Soc.* **1950**, *72*, 3185.
(39) Butler, A.; Danzitz, N. J. *J. Am. Chem. Soc.* **1987**, *109*, 1864.
(40) Vilter, H.; Rehder, D. *Inorg. Chim. Acta* **1987**, *136*, L7.
(41) Tracey, A. S.; Gresser, M. J.; Parkinson, K. M. *Inorg. Chem.* **1987**, *26*, 629.
(42) Rehder, D.; Weidermann, C.; Duch, A.; Priebsch, W. *Inorg. Chem.* **1988**, *27*, 584.

Contribution from the Department of Chemistry, McGill University, 801 Sherbrooke Street West, Montreal, Quebec, Canada H3A 2K6

# Synthesis and Characterization of the Disulfanoplatinum Complexes *cis*-$(PPh_3)_2Pt(phth)SSR$, Where phth = Phthalimido and R = $CH_2Ph$, $CH_2CH_2CH_3$, $CHMe_2$, *p*-$C_6H_4Me$, phth

Alan Shaver* and Rabin D. Lai

*Received March 14, 1988*

Disulfano complexes of the type *cis*-$(PPh_3)_2Pt(phth)SSR$, where phth = phthalimido and R = $CH_2Ph$, $CH_2CH_2CH_3$, $CHMe_2$, 4-$C_6H_4Me$, phth, have been prepared via oxidative addition of RSS(phth) to $(PPh_3)_2Pt(C_2H_4)$, wherein S-N bond cleavage occurs. Similarly, the thiolato analogues *cis*-$(PPh_3)_2Pt(phth)SR$ were obtained by using RS(phth). *cis*-$(PPh_3)_2Pt(phth)SSR$ complexes, where R = $CH_2Ph$, phth, are desulfurized by $PPh_3$ to give *cis*-$(PPh_3)_2Pt(phth)SCH_2Ph$ and *cis*-$(PPh_3)_2Pt(phth)_2$, respectively. Treatment of *cis*-$L_2Pt(SCH_2Ph)_2$, where L = $PPh_3$, $PMePh_2$, $PMe_2Ph$, with (phth)SS(phth) resulted in stepwise displacement of the phenylmethanethiolato ligands by phthalimido groups to give first *cis*-$L_2Pt(phth)SCH_2Ph$ and upon further reaction *cis*-$L_2Pt(phth)_2$ for L = $PPh_3$, $PMePh_2$ accompanied by the formation of organic polysulfanes $RS_xR$, where $x$ = 2-4. At -20 °C *trans*-$(PMe_2Ph)_2Pt(phth)SCH_2Ph$ was isolated. The complexes *cis*-$L_2Pt(phth)_2$ were also prepared from *cis*-$L_2PtCl_2$ and potassium phthalimide.

## Introduction

Organic sulfides, disulfides, and trisulfides are common and important species. While thiolato ligands ($RS^-$) are well-known,[1] simple disulfano ($RSS^-$) ligands are rare. In view of the propensity of sulfur to catenate, it would not be surprising if such species had an extensive chemistry with transition metals. Recently, a CuSSR species[2] and a $RSS^-$ ligand[3] bridging two molybdenum atoms were reported in model studies of copper enzymes and

(1) (a) Abel, E. W.; Crosse, B. C. *Organomet. Chem. Rev.* **1967**, *2*, 443. (b) Livingstone, S. E. *Q. Rev. Chem. Soc.* **1965**, *19*, 386.
(2) John, E.; Bharadwaj, P. K.; Krogh-Jespersen, K.; Potenza, J. A.; Schugar, H. J. *J. Am. Chem. Soc.* **1986**, *108*, 5015.
(3) Nobel, M. E. *Inorg. Chem.* **1986**, *25*, 3311.

0020-1669/88/1327-4664$01.50/0 